

*Electronic Supplementary Information (ESI)*

**Synthesis of a Conductive coordination polymer via a one pot thioether deprotect process**

Wenkai Liao,<sup>ab</sup> Siping Yin,<sup>ab</sup> Sha Wu<sup>ab</sup> and Wei Xu<sup>\*ab</sup>

a. Beijing National Laboratory for Molecular Sciences, Key Laboratory of Organic Solids, Institute of Chemistry, Chinese Academy of Sciences, Beijing 100190, China.  
E-mail: wxu@iccas.ac.cn.

b. University of Chinese Academy of Sciences, Beijing 100049, China.

## Table of Contents

<b>Section 1. Materials and Methods .....</b>	<b>3</b>
<b>Section 2. Synthetic Procedures .....</b>	<b>5</b>
<b>Section 3. Supplementary Figures .....</b>	<b>6</b>
<b>Section 4. Supplementary Tables .....</b>	<b>13</b>
<b>Section 5. Supplementary References .....</b>	<b>13</b>

## Section 1. Materials and Methods

### Materials

P-chloranil, NaH, dry tetrahydrofuran and ethylene glycol were purchased from J&K Scientific Co. Ltd.  $\text{NiCl}_2 \cdot 6\text{H}_2\text{O}$  was purchased from Energy Chemical Co. Ltd.  $\text{MnO}_2$  was purchased from Bide Pharmatech Ltd. Water was purified using the Milli-Q purification system. The solvents were degassed by the Freeze-Thaw method before using.  $(^t\text{BuS})_4\text{TTHQ}$  was synthesized by a modified method according to the previous literature.<sup>1</sup>

### Methods

**$^{13}\text{C}$ -NMR and  $^1\text{H}$ -NMR spectra.**  $^{13}\text{C}$ -NMR and  $^1\text{H}$ -NMR spectra were recorded at AVANCE  $\square$  HD 400MHz (Bruker). The chemical shifts were reported in parts per million (ppm) using the residual solvent signals as internal standards.

**Thermogravimetric analysis.** TGA data was collected on a PerkinElmer TGA 8000 instrument under nitrogen atmosphere.

**X-ray characterization.** Experimental PXRD data was collected on a PANalytical Empyrean II X-Ray diffractometer using Cu Ka irradiation ( $\lambda=1.5406 \text{ \AA}$ ). The generator was operated at 40 kV and 40 mA. Samples were scanned at diffraction angles ranging between  $2^\circ$  and  $60^\circ$  at a scanning rate of  $0.017^\circ/\text{s}$ .

**SEM Characterizations.** The SEM and EDS images were obtained using a Toshiba SU8020-SEM with an acceleration voltage of 10 kV.

**X-ray photon spectrum (XPS) and Ultraviolet photoelectron spectroscopy (UPS) characterizations.** XPS and UPS were performed with a monochromatic magnesium Ka source (1253.8 eV) using AXIS Ultra-DLD ultrahigh vacuum photoemission spectroscopy system (Kratos Co.).

**Fourier-transform infrared (FT-IR) spectroscopy characterizations.** The spectra data was collected on VERTEX 70v vacuum micro-Fourier infrared spectrometer.

**UV-vis-NIR spectrum.** The spectra were collected on a LAMBDA 1050+ spectrophotometer between 200 and 2500 nm under ambient environment. A  $\text{BaSO}_4$  background was collected prior to the sample measurement.

**Electrical property measurement.** The electrical conductivities were measured via a four-probe method by using a KEITHLEY 2002 Multimeter (Keithley Instrument Inc.). The temperature of measurement environment for electrical conductivity was controlled by a CTI Cryogenics refrigerator. The pellet was connected with four probes by conductive silver paste. The Seebeck coefficient was measured by the SB-100 Seebeck Measurement System (MMR Tech.).

**DFT calculation.** The AA stacking structure model in a CMMM space group, orthorhombic system was constructed. The Geometry optimization and band structure calculations were carried out using VASP package. The PBE exchange-correlation functional<sup>2</sup> with optB88 van der Waals (vdW) dispersion corrections<sup>3</sup> was employed. The plane wave energy cutoff was set to 550 eV. Uniform  $2 \times 2 \times 1$ ,  $2 \times 2 \times 7$  Monkhorst-Pack k-point meshes were employed for the monolayer and bulk crystal. For monolayer calculation a space of 15nm was inserted between the 2D layers to insulating the interlayer interaction. High-symmetry K-points in the first Brillouin Zone are illustrated in Figure S6. The optimized cell parameters are  $a = 23.307$ ,  $b = 14.354$ ,  $c = 3.400 \text{ \AA}$ ,  $\alpha = \beta = \gamma = 90^\circ$ , which is consistent with the cell parameters refined against the PXRD data. The corresponding atom coordinates are list in Table S2.

## Section 2. Synthetic Procedures

### Synthesis of (<sup>t</sup>BuS)<sub>4</sub>TTHQ.

In a three-necked flask, NaH (55% dispersion in oil, 1.5 equivalent per equivalent chlorine, 2.4g, 60mmol) was suspended in dry tetrahydrofuran (100 ml) after washed by n-hexane. After cooling to 0 °C, 2-methyl-2-propanethiole (2.2 equivalent per equivalent chlorine, 60mmol, 5.4g) was drop added with stirring (15 min). After addition, the reaction mixture is stirred at room temperature for 1 h, whereupon the p-chloranil (2.46g, 10mmol) is added. After reacting 24 h at 20 °C, the solution was quenched by water, extracted with ethyl acetate three times, dried with anhydrous sodium sulfate, dissolved in dichloromethane and recrystallized three times with methanol to obtain white powder. The yield was 2.8587g(30.9%). <sup>1</sup>H NMR(400 MHz, CDCl<sub>3</sub>): δ= 1.30 (s, 36H, CH<sub>3</sub>), 7.67 (s, 2H, OH). <sup>13</sup>C NMR(400 MHz, CDCl<sub>3</sub>): δ=31.68 (CH<sub>3</sub>), 51.10 (CMe<sub>3</sub>), 128.10 (C-2), 155.70 (C-1).

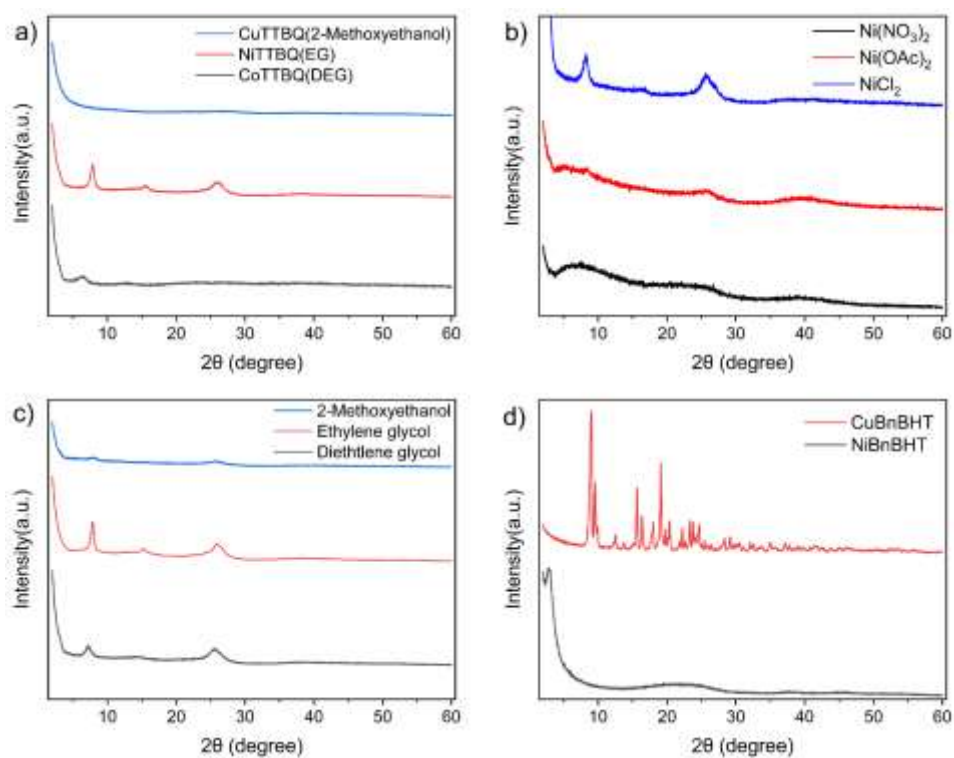
### Synthesis of (<sup>t</sup>BuS)<sub>4</sub>TTBQ.

(<sup>t</sup>BuS)<sub>4</sub>TTHQ(2.8587g) was dissolved in 50ml dichloromethane and MnO<sub>2</sub> (5.7174g, m(MnO<sub>2</sub>): m((<sup>t</sup>BuS)<sub>4</sub>TTHQ)=2) was add into the solution. The mixture was stirred for 2 hours. After filtration, the solution was removed by rotational evaporation. Crude product was recrystallized from a solution of dichloromethane: n-hexane=1: 10. A black crystal was obtained by filtration and washed with cold n-hexane. The solvents were removed under vacuum. The yield of (<sup>t</sup>BuS)<sub>4</sub>TTBQ was 2.1062g (71%). <sup>1</sup>H NMR (400 MHz, CDCl<sub>3</sub>): δ= 1.45 (s, 36H, CH<sub>3</sub>). <sup>13</sup>C NMR (400 MHz, CDCl<sub>3</sub>): δ=32.64 (CH<sub>3</sub>), 52.56 (CMe<sub>3</sub>), 152.75 (C-2), 178.89 (C-1). Anal. Calc. for C<sub>22</sub>H<sub>36</sub>O<sub>2</sub>S<sub>4</sub> (460.16): C, 57.35%; H, 7.88%; S, 27.83%. Found: C, 57.31%; H, 7.85%, S, 27.93%.

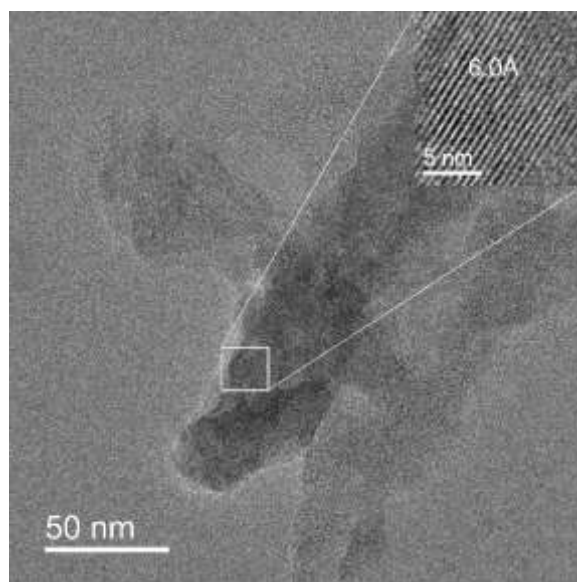
### Synthesis of Ni-TTBQ.

The powder of Ni-TTBQ was synthesized via a one-pot reaction of NiCl<sub>2</sub> and (<sup>t</sup>BuS)<sub>4</sub>TTBQ. NiCl<sub>2</sub>·6H<sub>2</sub>O (156.9mg, 0.66mmol) and (<sup>t</sup>BuS)<sub>4</sub>TTBQ (100mg, 0.22mmol) were dissolved in degassed ethylene glycol (60mL) and then heated to 120 °C and reacted overnight. After 12 hours, powder was obtained by filtration and washed three times with water, acetone and dichloromethane, respectively. And the solvents were removed under vacuum. The yield of Ni-TTBQ: 60mg, ~ 30%.

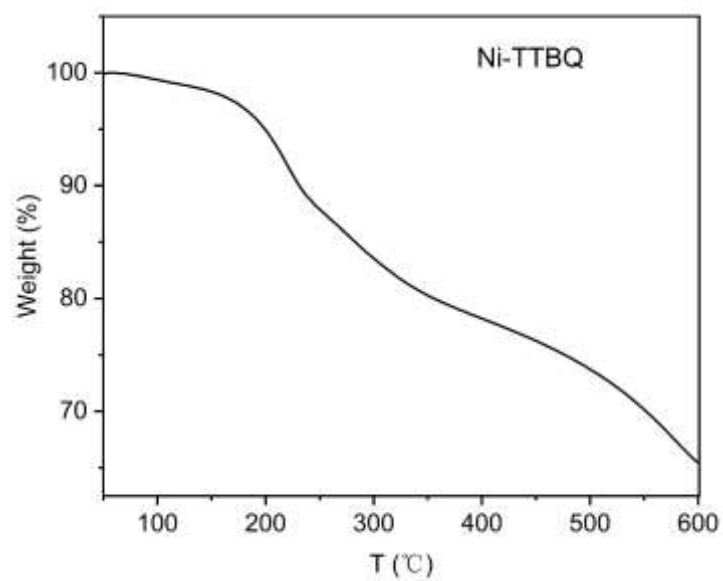
### Section 3. Supplementary Figures



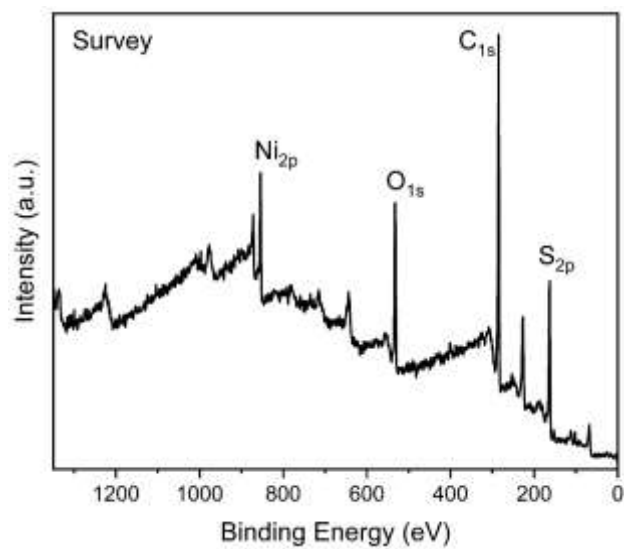
**Figure S1.** PXRD data of trials with a) different metal ions, b) metal salts, c) solvents and d) PXRD patterns of reaction product of 1,2,3,4,5,6-hexakis(benzylthio)benzene with  $\text{NiCl}_2$  and  $\text{CuCl}_2$ .



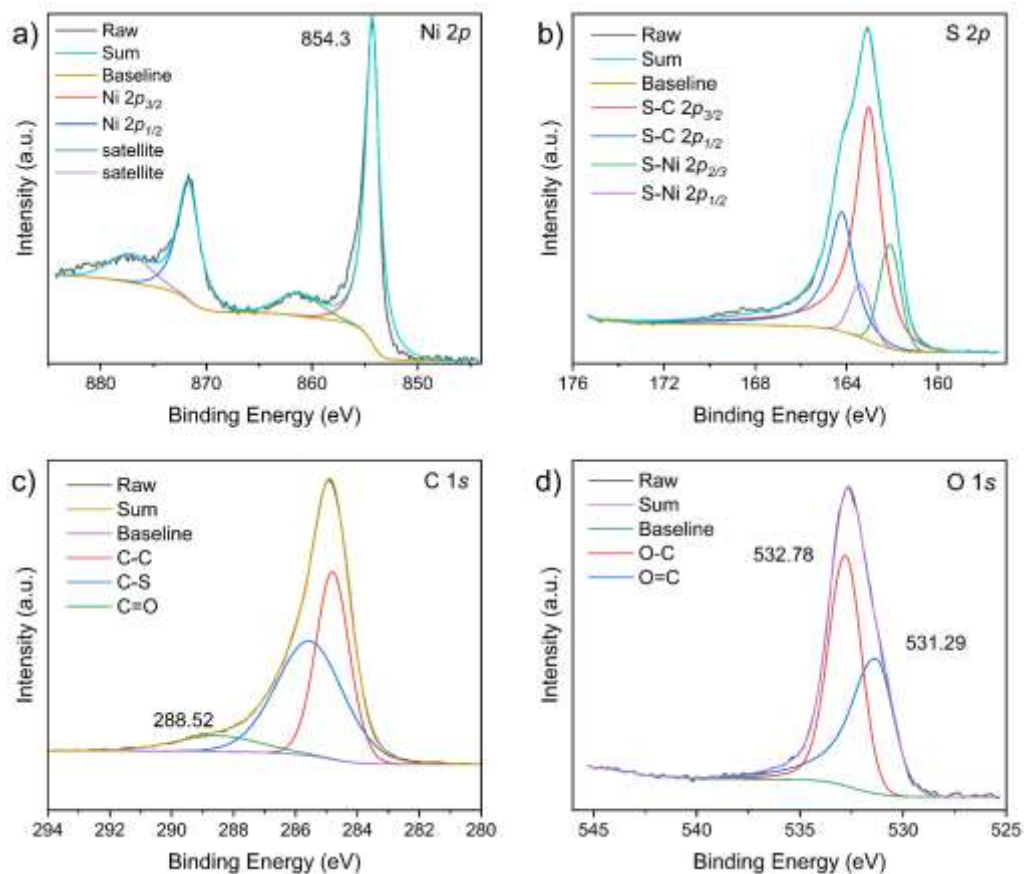
**Figure S2.** High-resolution TEM image of Ni-TTBQ.



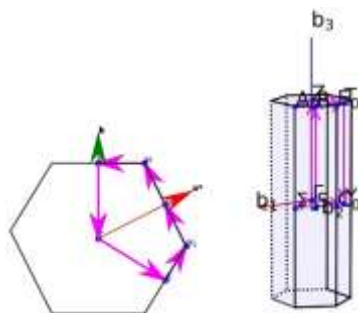
**Figure S3.** TGA data of Ni-TTBQ under nitrogen atmosphere.



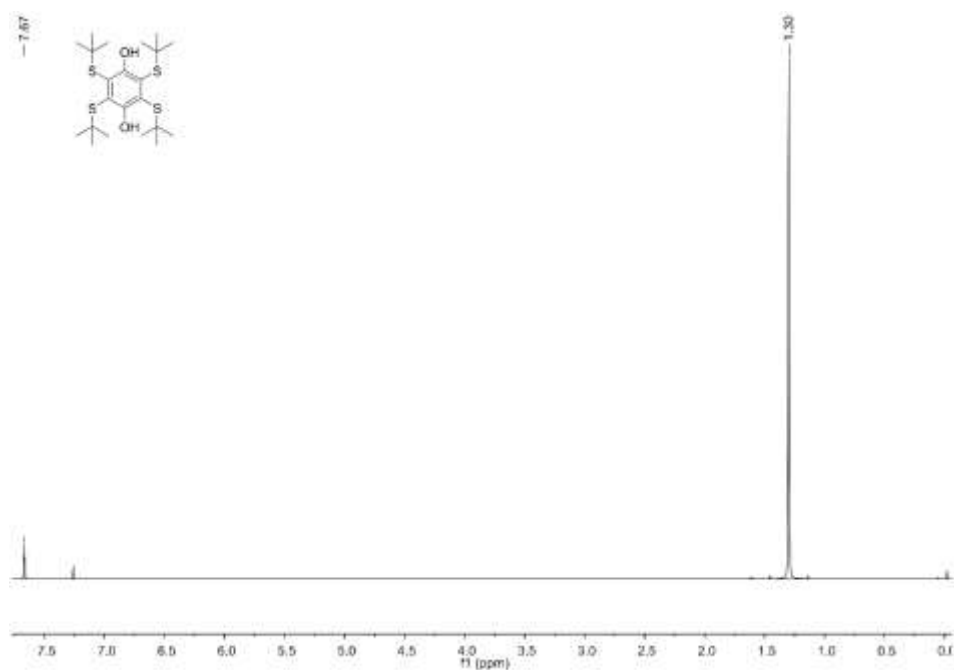
**Figure S4.** The full XPS spectrum of Ni-TTBQ.



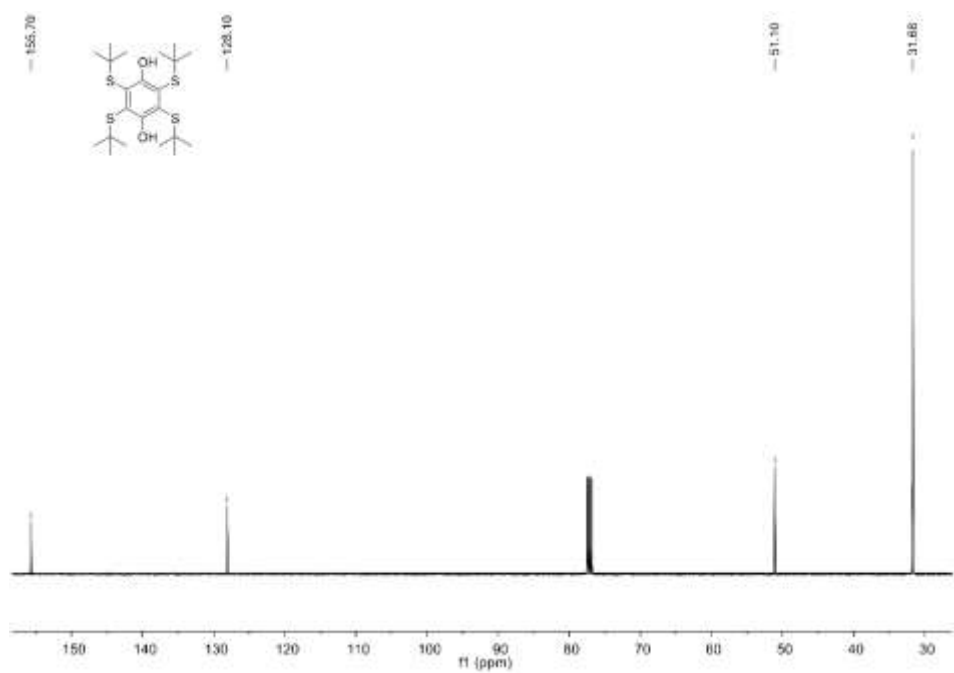
**Figure S5.** Fine XPS spectra of Ni-TTBQ. a) Ni 2p; b) S 2p; c) C 1s and d) O 1s spectra.



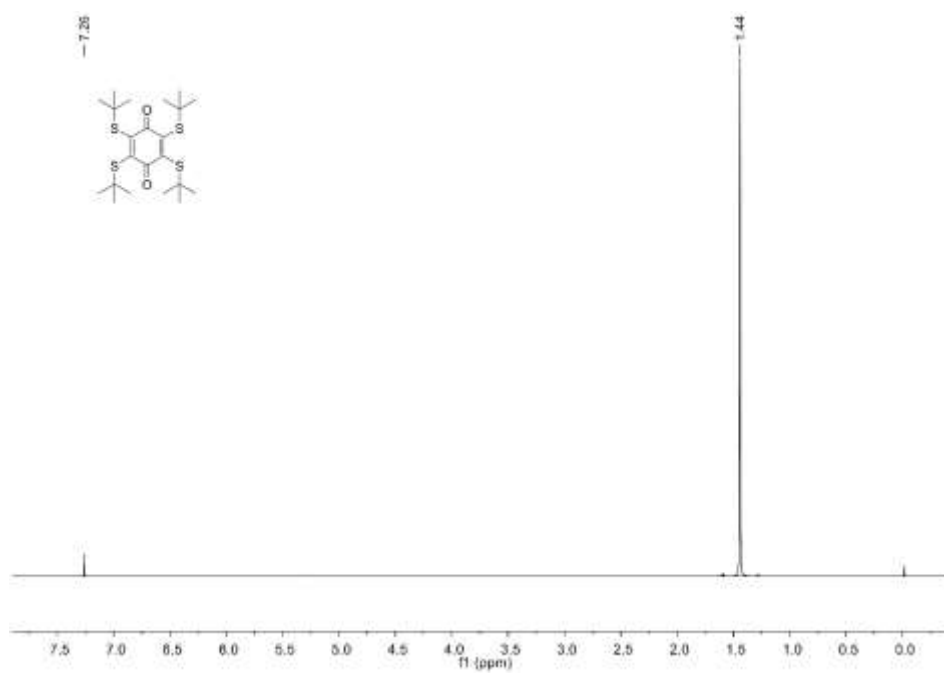
**Figure S6.** High K-points in the first Brillouin Zone for the monolayer lattice (left) and 3D crystal (right) of Ni-TTBQ.



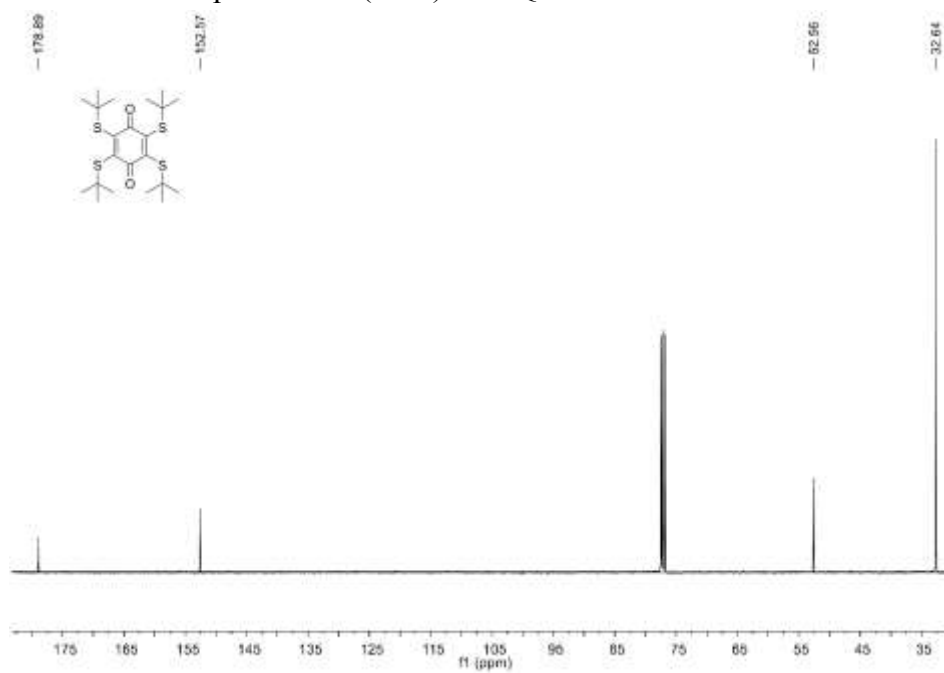
**Figure S7.**  $^1\text{H}$ -NMR spectrum of  $(t\text{BuS})_4\text{TTHQ}$ .



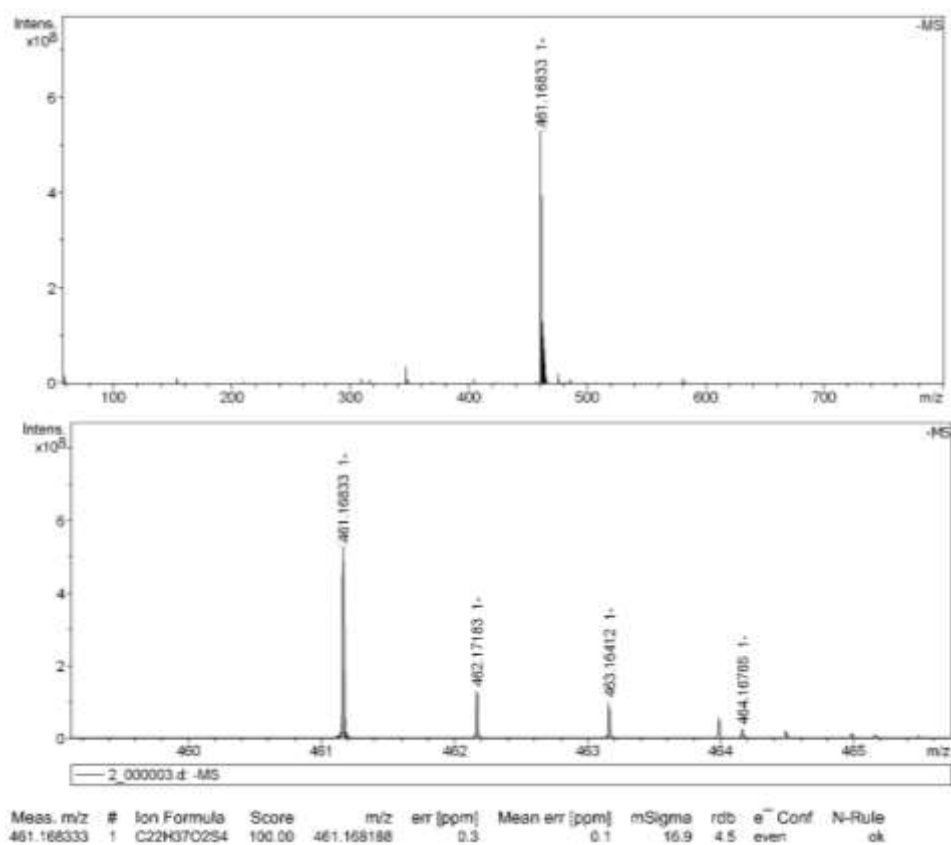
**Figure S8.**  $^{13}\text{C}$ -NMR spectrum of  $(t\text{BuS})_4\text{TTHQ}$ .



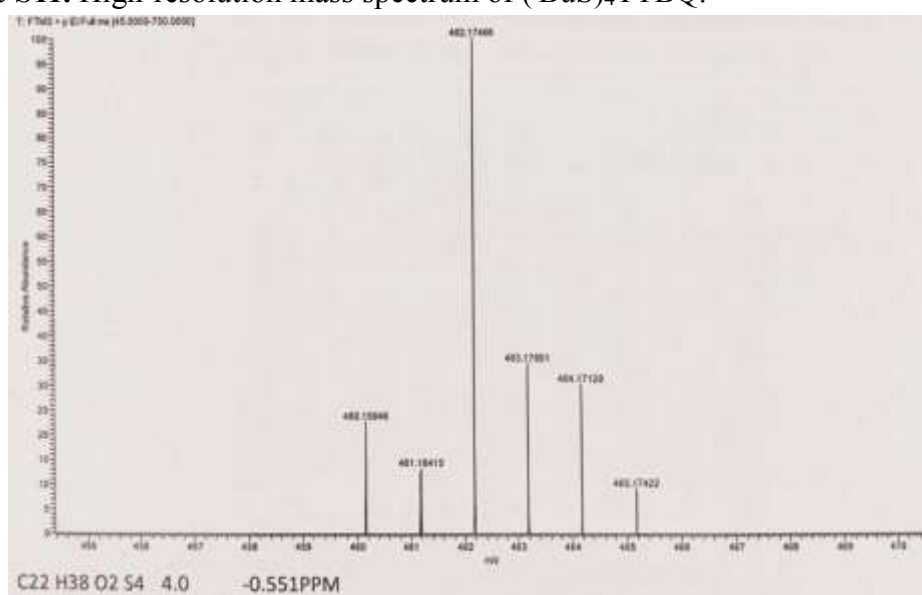
**Figure S9.**  $^1\text{H}$ -NMR spectrum of  $(t\text{BuS})_4\text{TTBQ}$ .



**Figure S10.**  $^{13}\text{C}$ -NMR spectrum of  $(t\text{BuS})_4\text{TTBQ}$ .



**Figure S11.** High-resolution mass spectrum of  $(^t\text{BuS})_4\text{TTBQ}$ .



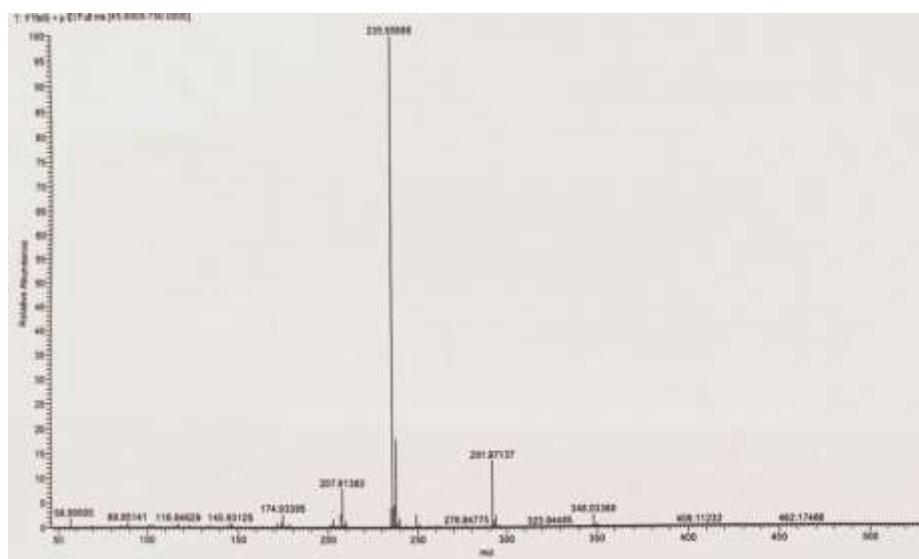


**Figure S12.** High-resolution mass spectrum of (tBuS)<sub>4</sub>TTHQ.

#### Section 4. Supplementary Tables

**Table S1.** Crystallographic data and results of the Le Bail refinement of AA stacking model of Ni-TTBQ against PXRD data.

Formula	Ni <sub>3</sub> C <sub>12</sub> S <sub>4</sub> O <sub>2</sub>
Formula weight/Z	630.73/2
Crystal system	orthorhombic
Space group	CMMM
<i>a</i> (Å)	23.503(10)
<i>b</i> (Å)	14.534(4)
<i>c</i> (Å)	3.3542(13)
$\alpha$ /°	90
$\beta$ /°	90
$\gamma$ /°	90
<i>V</i> (Å <sup>3</sup> )	1145.7(7)
R <sub>wp</sub>	1.88%
R <sub>p</sub>	1.46%

**Table S2.** Atomic coordinates of geometry optimized AA stacking model of Ni-TTBQ.

Atom	X	Y	Z
S1	0.706	0.382	0
S2	0.936	0.608	0
C1	0.766	0.450	0
C2	0.819	0.598	0
C3	0.873	0.549	0
O1	0.819	0.689	0
Ni1	0	0.5	0
Ni2	0.25	0.75	0

**Table S3. Comparison of electrical conductivity for representative 2D conductive coordination polymers.<sup>4</sup>**

Compound Formula	Conductivity /S cm <sup>-1</sup>	Ref
Cu-DBC	0.01, pellet	5
Cu-HAB	0.11 ± 0.03, pellet, 4-probe	6
Ni-HAB	0.7 ± 0.15, pellet, 4-probe	6
Co-HAB	1.57	7
Cu-HHB	7.3*10 <sup>-8</sup> -2.0*10 <sup>-6</sup> , pellet, van der Pauw	8
Ni-Pc	0.2, pellet, 4-probe	9
Fe-PTC	10, van der Pauw	10
Cu-HHTTP	2.4*10 <sup>-8</sup> , pellet, 4-probe	11
Ni-HHTTP	3.6*10 <sup>-4</sup> , pellet, 4-probe	11
Co-HHTTP	1.4*10 <sup>-3</sup> , pellet, 4-probe	11
Cu-HHTTP	0.2, crystal, 4-probe	12
Ni-HHTTP	0.01±0.003, pellet, 4-probe	13
Cu-HITP	0.2, pellet, 2-probe	14
	2, pellet, 2-probe; 50, pellet	14
Ni-HITP	40 (film, van der Pauw)	15
<b>Ni-TTBQ</b>	<b>0.02, pellet, 4-probe</b>	<b>This work</b>

## Section 5. Supplementary References

- 1 J. Becher, C. E. Stidsen, H. Toftlund and F. M. Asaad, *Inorganica Chimica Acta*, 1986, **121**, 23-26.
- 2 J. P. Perdew, K. Burke and M. Ernzerhof, *Physical Review Letters*, 1996, **77**, 3865-3868.
- 3 J. Klimeš, D. R. Bowler and A. Michaelides, *Physical Review B*, 2011, **83**, 195131.
- 4 J. Liu, Y. Zhou, Z. Xie, Y. Li, Y. Liu, J. Sun, Y. Ma, O. Terasaki and L. Chen, *Angewandte Chemie International Edition*, 2020, **59**, 1081–1086.
- 5 J. Liu, Y. Zhou, Z. Xie, Y. Li, Y. Liu, J. Sun, Y. Ma, O. Terasaki and L. Chen, *Angewandte Chemie International Edition*, 2020, **59**, 1081–1086.
- 6 D. Feng, T. Lei, M. R. Lukatskaya, J. Park, Z. Huang, M. Lee, L. Shaw, S. Chen, A. A. Yakovenko, A. Kulkarni, J. Xiao, K. Fredrickson, J. B. Tok, X. Zou, Y. Cui and Z. Bao, *Nature Energy*, 2018, **3**, 30-36.
- 7 J. Park, M. Lee, D. Feng, Z. Huang, A. C. Hinckley, A. Yakovenko, X. Zou, Y. Cui and Z. Bao, *Journal of the American Chemical Society*, 2018, **140**, 10315-10323.
- 8 J. Park, A. C. Hinckley, Z. Huang, D. Feng, A. A. Yakovenko, M. Lee, S. Chen, X. Zou and Z. Bao, *Journal of the American Chemical Society*, 2018, **140**, 14533–14537.
- 9 H. Jia, Y. Yao, J. Zhao, Y. Gao, Z. Luo and P. Du, *Journal of Materials Chemistry A*, 2018, **6**, 1188–1195.
- 10 R. Dong, Z. Zhang, D. C. Tranca, S. Zhou, M. Wang, P. Adler, Z. Liao, F. Liu, Y. Sun, W. Shi, Z. Zhang, E. Zschech, S. C. B. Mannsfeld, C. Felser and X. Feng, *Nature Communications*, 2018, **9**, 2637.
- 11 L. Mendecki, M. Ko, X. Zhang, Z. Meng and K. A. Mirica, *Journal of the American Chemical Society*, 2017, **139**, 17229-17232.
- 12 M. Hmadeh, Z. Lu, Z. Liu, F. Gándara, H. Furukawa, S. Wan, V. Augustyn, R. Chang, L. Liao, F. Zhou, E. Perre, V. Ozolins, K. Suenaga, X. Duan, B. Dunn, Y. Yamamoto, O. Terasaki and O. M. Yaghi, *Chemistry of Materials*, 2012, **24**, 3511–3513.
- 13 M. K. Smith, K. E. Jensen, P. A. Pivak and K. A. Mirica, *Chemistry of Materials*, 2016, **28**, 5264–5268.
- 14 M. G. Campbell, D. Sheberla, S. F. Liu, T. M. Swager and M. Dincă, *Angewandte Chemie International Edition*, 2015, **54**, 4349–4352.
- 15 G. Wu, J. Huang, Y. Zang, J. He and G. Xu, *Journal of the American Chemical Society*, 2017, **139**, 1360–1363.